



# 1 Identification of nighttime urban flood inundation extent using deep 2 learning

3 Jiaquan Wan<sup>1, 2, 3</sup>, Xing Wang<sup>4</sup>, Yannian Cheng<sup>5</sup>, Cuiyan Zhang<sup>4</sup>, Yufang Shen<sup>1, 2, 3</sup>, Fengchang Xue<sup>5</sup>,  
4 Tao Yang<sup>1, 2, 3</sup> and Quan J. Wang<sup>6</sup>

5 <sup>1</sup>College of Hydrology and Water Resources, Hohai University, Nanjing, 210098, China

6 <sup>2</sup>The National Key Laboratory of Water Disaster Prevention, Hohai University, Nanjing, 210098, China

7 <sup>3</sup>Yangtze Institute for Conservation and Development, Hohai University, Jiangsu, 210098, China

8 <sup>4</sup>School of Computer Engineering, NanJing Institute of Technology, Nanjing 211167, China

9 <sup>5</sup>School of Remote Sensing and Surveying Engineering, Nanjing University of Information Science & Technology, Nanjing  
10 210044, China

11 <sup>6</sup>Department of Infrastructure Engineering, Faculty of Engineering and Information Technology, The University of  
12 Melbourne, Victoria 3010, Australia

13 *Correspondence to:* Xing Wang (jwangxing0719@163.com)

14 **Abstract.** With the acceleration of urbanization, the disaster of urban flooding has had a serious impact on urban  
15 socio-economic activities and has become one of the important factors restricting social development in China. Accurate and  
16 timely identification of urban flooding extents is crucial for decision-making. Traditional remote sensing technologies are  
17 often limited by environmental factors, making them less suitable for application in complex urban terrains. The  
18 development of emerging technologies and the increase in urbanisation have led to a significant increase in the number of  
19 surveillance devices within cities, while the development of deep learning techniques has led to their widespread application  
20 in various fields. Deep learning methods using video images as a data source provide a new technical methods for  
21 intra-urban waterlogging recognition. However, current research mainly focuses on waterlogging recognition in daytime  
22 scenes, often ignoring nighttime, a time of high waterlogging incidence. To address these challenges faced by flooding  
23 recognition in the nighttime, this study proposes a deep learning model—NWseg—to achieve the recognition of the extent of  
24 waterlogging at night. Initially, we constructed a dataset of 4,000 images of nighttime urban flooding. Subsequently,  
25 MobileNetV2 and Resnet101 networks were used to replace the DeepLabv3+ backbone network and compared with the  
26 NWseg model. Next, the NWseg model is compared with ResNet50-FCN, LRASPP and U-Net models to evaluate the  
27 performance of different models in nighttime urban flooding identification. Finally, the applicability and performance  
28 differences of each model in specific environments were verified. In conclusion, this study successfully demonstrates the  
29 effectiveness of the NWseg model for nighttime urban flooding identification and provides new insights for nighttime urban  
30 flooding identification.

31 **Keywords:** Deep learning, Nighttime flooding identification, Urban flooding, NWseg



## 32 **1 Introduction**

33 In recent years, extreme rainfall events have been occurring frequently in the context of complex climate change.  
34 Concurrently, with the acceleration of urbanization processes, the proportion of impervious surfaces has been continuously  
35 expanding, resulting in serious urban flooding issues in many cities worldwide (Xue et al., 2023). Urban flooding often  
36 coincides with multiple compounded disasters and may even trigger secondary calamities, posing serious threats to the safety  
37 of urban residents, the normal operation of city functions, and sustainable development. This exacerbates the vulnerability of  
38 urban socio-economic system (Luo et al., 2020). Therefore, achieving real-time and effective monitoring of urban flooding  
39 has become a critical issue that urgently needs to be addressed.

40 Remote sensing technology has made significant advancements in the field of urban flood monitoring, providing new  
41 perspectives for flood disasters identification through high spatial, temporal and spectral resolution data (Hao., 2022).  
42 However, despite its excellent performance at the macro scale, remote sensing technology has limitations in urban area  
43 monitoring. Due to insufficient temporal resolution as well as the influence of cloud cover and changing atmospheric  
44 conditions, remote sensing techniques have difficulty in capturing subtle topographic changes within cities, and are unable to  
45 monitor fast-changing flooding events in real time (Gao., 2023). In addition, the complexity of the urban environment,  
46 especially the dynamic changes of small-scale water bodies and localized waterlogging, further increases the difficulty of  
47 remote sensing technology in urban flood monitoring. Therefore, an intelligent and real-time urban flood monitoring method  
48 is urgently needed to achieve more precise flood identification.

49 With technological advancements, the emerging fields of deep learning and computer vision have matured and engaged in  
50 interdisciplinary collaborations, achieving remarkable results that offer new technical approaches for urban flood  
51 identification. Particularly in image recognition, deep learning's advantages in extracting global features and contextual  
52 information make it highly promising for inundation detection (Liao., 2023). Simultaneously, the increasing level of  
53 urbanization has led to the widespread deployment of video surveillance devices across urban areas, particularly along city  
54 roads, where they are ubiquitous. During rainfall, these cameras can fully record the flooding process, providing real-time  
55 reflections of road inundation changes (Wang et al., 2024; Yang et al., 2022; Cheng et al., 2018). Therefore, combining deep  
56 learning with traffic cameras can effectively achieve real-time recognition of urban flooding.

57 Existing research has demonstrated that deep learning excels in segmenting inundated areas. (Bai et al., 2021) utilized the  
58 YOLOv2 object detection model to extract water accumulation features from images collected by Xi'an University of  
59 Science and Technology, achieving an average recognition accuracy of over 85% through multiple model training sessions,  
60 demonstrating the precision of this method for inundation area extraction. (Wang et al., 2021) classified road images into  
61 four categories—background, dry surface, inundated area, and slippery surface—and used the Res-UNet+ semantic  
62 segmentation network to handle different lighting and scene conditions, achieving an Mean Intersection over Union (MIoU)



63 of 90.07%, outperforming traditional classification methods. (Sarp et al., 2020) applied the Mask R-CNN model to  
64 automatically detect and segment floodwaters in urban, suburban, and natural scenes, achieving 99% accuracy in the  
65 detection phase and 93% in the segmentation phase. (Sazara et al., 2019) used a deep learning approach to detect standing  
66 water on urban roads, in which a pre-trained VGG-16 network was used in the classification phase and a full convolutional  
67 neural network was used in the segmentation task, and compared it with the traditional classifier and extraction algorithms  
68 with manually-designed features, and the results showed that the deep learning approach has a more obvious advantage in  
69 both the recognition and segmentation of standing water. However, current research focuses on daytime scenes, and the  
70 existing datasets lack diversity to cover flooding scenes at night or under complex weather conditions. Meanwhile, some  
71 algorithms underperform when processing images in low-light or adverse conditions, making flood identification at night or  
72 in challenging weather a technical challenge. This limitation underscores the urgent need for accurate nighttime flood  
73 monitoring and the necessity for algorithm improvements and dataset expansion.

74 For this specific scenario, we propose the NWseg model for waterlogging recognition in nighttime, inspired by the  
75 method introduced by (Wei et al., 2023). The problem of insufficient model recognition accuracy in nighttime scenes is  
76 effectively solved by two core components, Semantic-Oriented Disentanglement (SOD) and Illumination-Aware Parser  
77 (IAParser) (Wei et al., 2023). On this basis, this study constructs an urban flooding dataset for nighttime scenarios, based on  
78 which the model is trained to improve the model's ability to recognise the extent of urban flooding in nighttime  
79 environments.

80 This study aims to enhance urban flood extent recognition in nighttime scenes by utilizing advanced semantic  
81 segmentation techniques and a comprehensive all-nighttime dataset, addressing the current limitations in both datasets and  
82 methodologies. More specific, our aims are as follows:

83 (1) Contributed a method for assessing urban flooded areas based on urban surveillance cameras in response to common  
84 challenges in the field of nighttime urban flooding identification.

85 (2) A comprehensive and representative nighttime urban flooding dataset is constructed. It covers a wide range of  
86 nighttime scenes, including different weather conditions and city layouts, providing a rich resource for training and testing  
87 semantic segmentation models.

88 (3) Replacement of the original DeepLabv3+ model network backbone with MobileNetV2 and Resnet101 networks is  
89 used to verify the performance impact of different network backbones on the DeepLabV3+ model through ablation  
90 experiments.

91 (4) A waterlogging recognition model NWseg for nighttime scenarios is contributed, and the significant advantages of the  
92 model in terms of robustness, effectiveness and practicality are verified by comparing with other existing models, which  
93 advances the research and development of nighttime urban flood recognition.



94 **2 Model**

95 **2.1 Nighttime Urban Segmentation Model**

96 Nighttime scenes are typically characterized by low-temperature illumination and complex artificial light sources, which lead  
97 to changes in object appearance due to variations in lighting conditions. This reinforces the entanglement between light  
98 invariant reflectance and light-specific illumination, making it challenging to extract discriminative features for semantic  
99 segmentation. Based on this background, proposed a nighttime waterlogging recognition model —NWseg, specifically  
100 designed to cope with the problem of degraded segmentation performance due to insufficient illumination and complexity in  
101 nighttime scenes (Wei et al., 2023).

102 The paradigm consists of two core steps: decoupling and parsing. The inference is shown in Figure 1. In the decoupling  
103 phase, NWseg decomposes the input image into light-invariant reflectance and illumination-specific components. The  
104 designed SOD framework decomposes the image into illumination-independent reflectance components and light-specific  
105 components by semantically supervising the training of the de-entanglement module. It utilises Retinex theory to ensure that  
106 stable light-invariant reflectance is extracted under complex illumination conditions, which enhances the semantic  
107 recognition in the subsequent parsing phase. The parsing phase then extracts illumination features using an  
108 Illumination-Aware Parser (IAParser), which quantitatively evaluates the semantic information contained in the illumination  
109 by using a pyramid pooling module and a convolutional layer to construct an attention mask. The final segmentation result is  
110 obtained by combining reflectance and illumination features. The model effectively copes with the complex and variable  
111 lighting challenges in nighttime scenes through the dual mechanism of decoupling and parsing, and significantly improves  
112 the performance of semantic segmentation (Wei et al., 2023).



113  
114 **Figure 1: NWseg model inference process**

115 **2.2 Typical semantic segmentation model**

116 The DeepLab network series is an improved set of models based on fully convolutional neural networks (FCNs). These  
117 methods effectively enhance the receptive field of convolutional kernels to acquire multi-scale feature information, thereby  
118 optimizing the spatial accuracy of segmentation results (Feng et al., 2023; Chen et al., 2024). The network models mainly  
119 utilize techniques such as atrous convolution and atrous spatial pyramid pooling (ASPP) to extract multi-scale features and



120 capture contextual information from images. The series includes DeepLabV1, DeepLabV2, DeepLabV3, and DeepLabV3+.  
121 DeepLabV3+ is the latest version in the DeepLab series (Li et al., 2024; Peng et al., 2024; Ma et al., 2024; Zhang et al.,  
122 2023); it introduces an encoder-decoder structure by adopting DeepLabV3 as the encoder and adding a decoder to form a  
123 new model. The Xception model is applied to the segmentation task, extensively using depthwise separable convolutions  
124 within the model. However, this network still has limitations in modeling long-range dependencies, insufficient handling of  
125 class-imbalanced data, and higher latency for real-time applications. While DeepLabV3+ combines the spatial pyramid  
126 pooling module and encoder-decoder structure in deep neural networks to achieve fine segmentation of object boundaries, it  
127 remains constrained in modeling long-range dependencies, dealing with class imbalance, and reducing latency for real-time  
128 applications (Li et al., 2023; Zhang et al., 2024; Tao et al., 2023).

129 To enhance the segmentation performance of DeepLabV3+ in urban flood scenes, this study designed ablation  
130 experiments to verify the effectiveness of different backbone networks and compared them with the NWseg model. First,  
131 experiments were conducted on the original, unmodified DeepLabV3+ network as a baseline model. Then, we replaced the  
132 original DeepLabV3+ backbone network with the lightweight MobileNetV2, constructing an improved model (denoted as  
133 MobileNetV2-DeepLabV3+). MobileNetV2 optimizes the number of model parameters by introducing a linear bottleneck  
134 layer and inverted residual structures, ensuring a lightweight model while maintaining high accuracy (Jin et al., 2023).  
135 Finally, we replaced the backbone network of DeepLabV3+ with the residual neural network ResNet101 to form another  
136 improved model (denoted as ResNet101-DeepLabV3+). ResNet101 leverages a residual learning mechanism, allowing input  
137 information to bypass certain layers, addressing gradient vanishing and explosion issues during deep network training. This  
138 enhances the model's ability to capture spatial depth and details, ultimately improving the accuracy and robustness of flood  
139 area recognition (Yang et al., 2023; Wang et al., 2024).

140 The Fully Convolutional Network (FCN) is an architecture specifically designed for semantic segmentation by replacing  
141 the fully connected layers of traditional Convolutional Neural Networks (CNNs) with convolutional layers. This allows  
142 FCNs to process input images of arbitrary sizes and perform accurate pixel-wise classification. FCNs extract features  
143 through convolutional layers, reduce feature dimensionality via pooling layers, and restore feature map sizes using  
144 upsampling layers, achieving precise pixel-level segmentation. Techniques such as bilinear interpolation are employed to  
145 preserve image details (Zhao et al., 2018). Additionally, skip connections in FCNs effectively fuse shallow and deep feature  
146 information, improving segmentation accuracy. In this study, ResNet50 is adopted as the backbone network for FCN,  
147 denoted as ResNet50-FCN. ResNet50 utilizes a residual learning mechanism to address gradient vanishing issues during  
148 deep model training, maintaining training stability and efficiency while enabling greater depth. The multiple residual blocks  
149 in ResNet50 capture rich multi-scale features, adapting to structures from coarse to fine. Its skip connections preserve the  
150 detailed information that can be lost during upsampling, ensuring high-precision semantic segmentation. Combining the



151 depth of ResNet50 with the flexibility of FCN, this model enhances the accurate detection of inundated areas in complex  
152 environments.

153 The LRASPP network is a lightweight semantic segmentation model designed for efficient operation on  
154 resource-constrained devices such as mobile and embedded systems. It simplifies the classic ASPP (Atrous Spatial Pyramid  
155 Pooling) module, retaining its ability to capture multi-scale contextual information while significantly reducing  
156 computational complexity and memory usage. By leveraging depthwise separable convolutions to reduce the number of  
157 parameters and incorporating detailed information from lower-level features, LRASPP achieves a balance between model  
158 efficiency and accuracy. The model employs MobileNetV3 as the lightweight backbone to extract image features and  
159 generate multi-scale feature maps. It also simplifies the original ASPP module by capturing multi-scale contextual  
160 information through atrous convolutions and fusing low-level detailed features to improve segmentation accuracy. By  
161 reducing convolutional layers and the number of channels, the network significantly lowers computational complexity. The  
162 final output is upsampled to match the input image size, ensuring both efficiency and accuracy in segmentation tasks (Tang  
163 et al., 2024).

164 U-Net is a classic network architecture for image segmentation, built on fully convolutional networks (FCNs). It utilizes  
165 skip connections to directly concatenate features from downsampling and upsampling layers along the channel dimension,  
166 effectively integrating information from different layers. U-Net features a symmetrical encoder-decoder structure, with a left  
167 downsampling path, a right upsampling path, and intermediate skip connections. The downsampling path resembles  
168 traditional CNN architectures, consisting of alternately stacked convolutional and pooling layers, while the upsampling path  
169 uses transposed convolution to progressively restore the feature maps to the original image resolution (Zhang et al., 2023).  
170 Shallow features primarily capture fine-grained information such as flood area edges, texture, and pixel position distribution,  
171 while deeper features extract more abstract, coarse-grained semantic information, helping solve the final pixel-level  
172 classification problem. U-Net's structural characteristics enable it to effectively handle detailed information in low-light  
173 environments, making it particularly suitable for nighttime flood detection and other low-light image segmentation tasks  
174 (Yadabendra et al., 2022).

175 We conducted comparative experiments on the FCN, LRASPP, U-Net, and NWseg models, evaluating their performance  
176 using metrics such as Precision, Recall, Mean Intersection over Union (MIoU), and F1 Score. All models were initialized  
177 with pretrained weights for their backbone networks and trained on the nighttime urban flooding dataset. The models were  
178 then evaluated on the test set, with relevant metrics calculated to determine the most suitable model for nighttime urban  
179 flood recognition.



180 **3 Design of experiments**

181 **3.1 Construction of dataset**

182 In this study, we employed web crawler technology using Google Chrome to construct a comprehensive nighttime urban  
183 waterlogging dataset by searching with the keyword "nighttime urban flooding." This dataset contains 4,000 images that  
184 capture a wide range of nighttime waterlogging scenes, varying in extent and shape. To enhance the dataset's robustness and  
185 comprehensiveness, we included images of complex scenes, such as strong lighting conditions and splashes caused by  
186 vehicles, ensuring its applicability to diverse nighttime flooding situations. During the data selection process, careful  
187 attention was given to the representativeness and balance of waterlogged areas across different scales, ranging from localized  
188 ponding to large-scale flood events, to ensure broad coverage of possible urban flooding conditions.

189 In addition, we performed the labeling work on the 4000 images in the dataset using the Labelme tool, which accurately  
190 extracted the waterlogged regions in each image. To further improve the accuracy of the annotations, we specifically  
191 assigned three graduate students to rigorously review and calibrate the boundary annotations for quality assurance. The  
192 annotation results are saved as labeled images. Figure 2 presents a comparison between the original images and the labeled  
193 images, where the waterlogged areas are marked in white and the non-waterlogged areas are marked in black.

194



195

196 **Figure 2: Data Samples**

197 **3.2 Evaluation metrics**

198 In validation and testing, mean Intersection over Union (MIoU), F1score, precision and recall were used to assess the  
199 performance of the semantic segmentation models (Jin et al., 2024).

200 The MIoU value is defined as the ratio of the intersection area of the predicted bounding box and the real bounding box to  
201 the concatenation area, and is calculated by averaging the results for each category. It is used to evaluate the accuracy of the  
202 location information of the predicted results of the target detection task. The larger the overlap area between the real and the  
203 presumed area of the object, the larger the calculated value of MIoU, and the more accurate the presumed target area. The  
204 calculation of the MIoU value follows the following formula:



$$MIoU = \frac{1}{k+1} \sum_{i=0}^k \frac{TP}{TP + FP + FN}$$

205 (1)

206 Precision, which is the proportion of samples predicted to be positive that are actually positive, is also known as the check  
207 rate, and can be expressed by the following formula:

$$Precision = \frac{TP}{TP + FP}$$

208 (2)

209 Recall, which is the proportion of actual positive samples that are predicted to be positive, is also known as the check all  
210 rate, and is given by the following formula:

$$Recall = \frac{TP}{TP + FN}$$

211 (3)

212 F1score is the reconciled mean of precision and recall. The formula for each precision evaluation metric is as follows:

$$F1score = \frac{2 \times Precision \times Recall}{Precision + Recall}$$

213 (4)

214 In the above formula, TP is the number of actual situations that are true and predicted to be true; FP is the number of  
215 actual situations that are false and predicted to be true; FN is the number of actual situations that are true and predicted to be  
216 false; and TN is the number of actual situations that are false and predicted to be false.

### 217 3.3 Experimental configuration

218 All experiments were conducted using an operating system of Windows 10, a CPU model of  
219 Intel(R)Core(TM)i712700F@2.10GHz, a GPU model of NVIDIA GeForce RTX3080, 32GB of operating memory,, a  
220 programming language of Python 3.13, and a deep learning framework of PyTorch1.13, GPU acceleration libraries are  
221 CUDA11.7, CUDNN8.4.1. the input image resolution is 512\*512 pixels, the training optimizer type is Adam, the weight  
222 decay index is 0.0001, and the initialized learning rate is 0.005. Parameters are shown in the Table 1.

223 **Table 1. Configuration table of the experiment**

Project	Model
Operating System	Windows 10
Programming Language	Python3.13
GPU	NVIDIA GeForce RTX3080
GPU memory	32GB



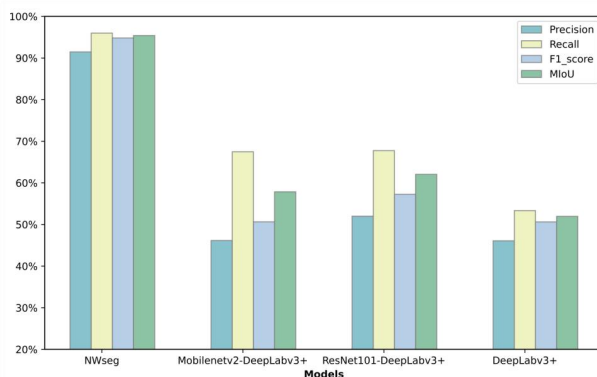


224 **4 Result**

225 **4.1 Ablation study**

226 **Table 2. NWseg and DeepLabv3+ series model training results**

Models	P/%	R/%	F1score	MIoU/%
MobileNetV2-DeepLabv3+	67.46	50.64	57.85	46.15
ResNet101-DeepLabv3+	67.74	57.24	62.05	51.98
DeepLabv3+	53.34	50.61	51.94	46.07
NWseg	95.99	94.8	95.39	91.46



227

228 **Figure 3. Comparison of experimental results between NWseg and DeepLabv3+ series of models**

229 In this section, we present a comparative analysis of the DeepLabV3+ model with different backbone networks and compare  
230 it with the NWseg model. As shown in Table 2 and Figure 3, replacing the original backbone of DeepLabV3+ with  
231 MobileNetV2 resulted in improvements across all evaluation metrics. Precision and F1score increased significantly by  
232 14.12% and 5.91%, respectively, while Recall and MIoU saw marginal improvements of 0.03% and 0.08%. When  
233 ResNet101 was used as the backbone, the model's performance improved even more, with Precision, F1 score, Recall, and  
234 MIoU increasing by 14.4%, 10.11%, 6.63%, and 5.91%, respectively. Despite these improvements, all three DeepLabV3+  
235 models still exhibited a noticeable performance gap compared to the NWseg model. The NWseg model significantly  
236 outperforms the other models by achieving 95.99%, 94.8%, 95.39%, and 91.46% in Precision, Recall, F1 score, and MIoU,  
237 respectively.

238 Overall, the use of MobileNetV2 as the backbone network of DeepLabV3+ significantly improves the evaluation indexes  
239 of the model while maintaining the lightweight, and MobileNetV2 successfully optimizes the computational efficiency and  
240 reduces the consumption of computational resources, but its performance is far inferior to that of the NWseg model. The deep  
241 network structure and advanced residual connection mechanism of ResNet101 make it perform more outstandingly in all  
242 evaluation indexes. In contrast, ResNet101, with its deep network structure and advanced residual connection mechanism,  
243 outperformed other backbones in all evaluation metrics, considerably boosting the overall performance of DeepLabV3+.  
244 Nevertheless, even with ResNet101, the DeepLabV3+ models still lag behind the NWseg model, indicating there is  
245 substantial room for further improvement in performance.

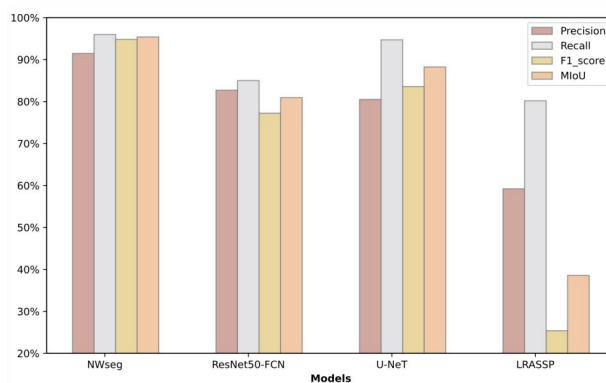


246 **4.2 Model performance experiments**

247 **Table 3.** NWseg and other segmentation model training results

Models	P/%	R/%	F1score	MIoU/%
NWseg	95.99	94.8	95.39	91.46
ResNet50-FCN	85	77.23	80.93	82.7
Lraspp	80.17	25.39	38.57	59.21
U-Net	94.7%	83.57	88.24%	80.5%

248



249

250 **Figure 4.** Comparison of experimental results between NWseg and other segmentation models

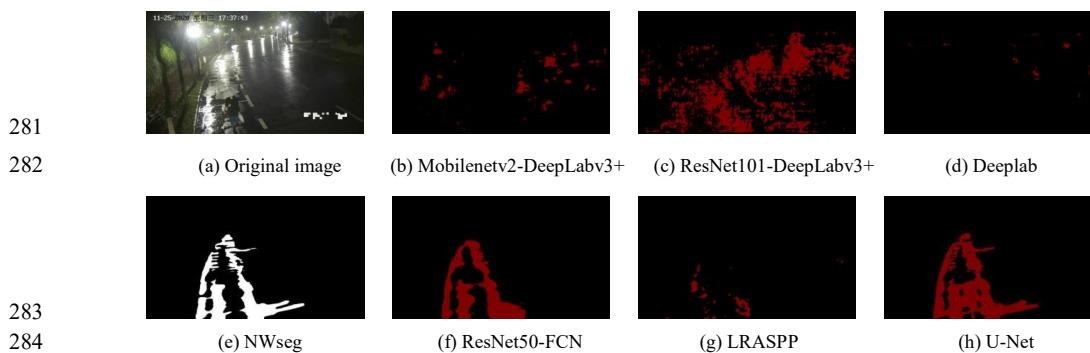
251 In this section, we present a comparative analysis of the experimental results of the NWseg model against other segmentation  
252 models. As shown in Table 3 and Figure 4, the NWseg model achieved optimal results on the test set of the social inundation  
253 dataset, with a Precision of 95.99%, Recall of 94.8%, F1-score of 95.39%, and MIoU of 91.46%. These metrics are  
254 significantly higher than those of the other models, demonstrating exceptional accuracy and recall rates. Compared to the  
255 ResNet50-FCN model, the NWseg model exhibits superior performance across all indicators, with increases of 10.99% in  
256 Precision, 17.57% in Recall, 14.46% in F1-score, and an 8.76% improvement in MIoU. When compared with the U-Net  
257 model, while the NWseg's Precision is similar, it outperforms in other metrics, with Recall, F1-score, and MIoU higher by  
258 11.23%, 7.15%, and 10.96% respectively. Additionally, compared to the lightweight LRASPP model, the NWseg model  
259 shows more pronounced advantages, with Precision increased by 15.82%, Recall significantly increased by 69.41%,  
260 F1-score improved by 56.82%, and MIoU enhanced by 32.25%. The lightweight design of LRASPP limits its ability to  
261 precisely capture details and edges, resulting in lower overall recognition accuracy.

262 Overall, the NWseg model demonstrates superior performance across all evaluation metrics and also shows strong  
263 performance in real scenario tests. In contrast, although the ResNet50-FCN model performs well in precision and detail  
264 processing, it lacks efficacy in handling edge regions, leading to slightly insufficient performance in complex scenes. While  
265 LRASPP offers advantages in computational efficiency due to its lightweight design, it has limitations in the precise capture  
266 of details and boundaries. The U-Net model is comparable to NWseg in accurately detecting target areas but is somewhat  
267 less robust and consistent when processing complex scenes.



### 268 4.3 Real-world scenes prediction comparison

269 To validate the effectiveness and stability of each model under challenging scenes, we conducted tests on seven models  
270 using nighttime rainfall scenes and nighttime strong illumination scenes (Liang et al., 2023). As shown in Figure 5(a)  
271 presents the original scene where streetlights at night generate strong reflections and halos on the water surface. Additionally,  
272 the intense lighting affects the detailed features of the ground. By comparing the recognition results of each model, it is  
273 evident that the NWseg, ResNet50-FCN, and U-Net models accurately detected the flooding conditions in the scene. Notably,  
274 the NWseg model exhibited a more refined recognition ability in identifying water accumulation in road depressions.  
275 However, both ResNet50-FCN and U-Net showed certain false detections when recognizing the overall flooded areas. In  
276 contrast, the Mobilenetv2-DeepLabv3+, DeepLab, and LRASPP models could only sporadically identify small flooded  
277 regions and exhibited varying degrees of false detections. Although the ResNet101-DeepLabv3+ model recognized a larger  
278 flooded area, a comparison with the original image reveals a relatively high false detection rate, indicating deviations in  
279 prediction accuracy. Overall, the NWseg model outperformed the others in this scene recognition task, demonstrating  
280 superior capability in recognizing flooded areas under complex lighting conditions.



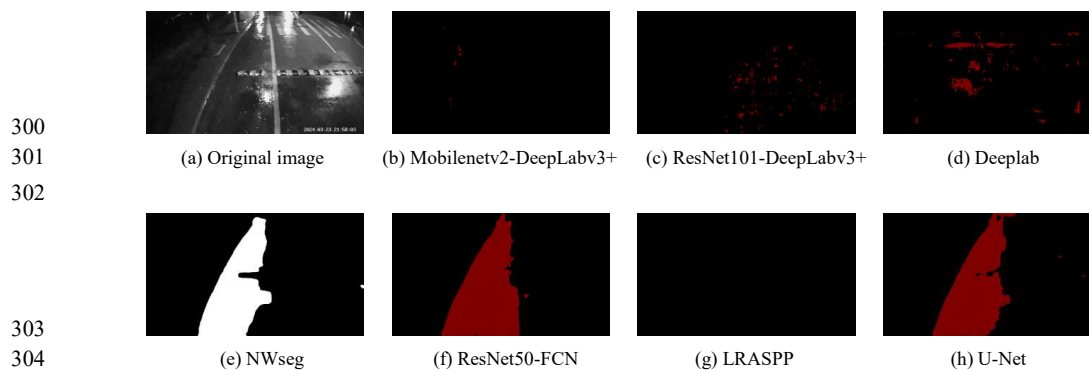
285 **Figure 5. Examination of nighttime strong illumination scenes**

286 Furthermore, in the nighttime rainfall scene tests, we evaluated each model's performance to simulate urban flood  
287 recognition under real-world conditions (Tan et al., 2021). In such scenes, reflections from rainwater, slippery road surfaces,  
288 and interference from raindrops on the camera lens can adversely affect image clarity and the models' recognition accuracy.  
289 As shown clearly in Figure 6, the NWseg, ResNet50-FCN, and U-Net models were able to correctly identify the flooded  
290 areas in the images, with the NWseg model providing the most detailed performance by accurately capturing the edges of the  
291 flooded regions. While ResNet50-FCN and U-Net also identified the extent of flooding relatively well, they were somewhat  
292 insufficient in recognizing the flood boundaries and exhibited some false detections.

293 In contrast, the other four models performed relatively poorly. Specifically, the LRASPP and  
294 Mobilenetv2-DeepLabv3+ models were almost unable to detect the flooding, indicating weaker recognition capabilities in  
295 nighttime rainfall scenes. Although ResNet101-DeepLabv3+ and DeepLab could detect some flooded areas, comparison



296 with the original images revealed that the regions identified did not accurately reflect the actual flooding conditions and had  
297 high false detection rates. Through comparative analysis, we further confirmed the challenges posed by nighttime rainfall  
298 environments for urban flood recognition and demonstrated the superior performance of the NWseg model in handling  
299 complex conditions such as nighttime rainfall.



303  
304  
305 **Figure 6. Examination of nighttime rainfall scenes**

## 306 **5 Conclusions**

307 This study addresses the technical challenges of nighttime urban flood detection by evaluating the performance of seven  
308 different models (Wan et al., 2024). First, we constructed a representative dataset comprising 4,000 images of nighttime  
309 urban flooding scenes, covering various nighttime environments and diverse urban backgrounds. Second, a model for  
310 nighttime waterlogging recognition, NWseg, is proposed to address the limitations in nighttime waterlogging recognition due  
311 to insufficient lighting and complex lighting conditions. Furthermore, we replaced the backbone networks of the  
312 DeepLabV3+ model with MobileNetV2 and ResNet101 and conducted ablation experiments to validate the performance of  
313 DeepLabV3+ with different backbones in nighttime flood recognition. We also performed a comparative analysis between  
314 these DeepLabV3+ models and the NWseg model, as well as systematically analyzed the NWseg, ResNet50-FCN, U-Net,  
315 and LRASPP models. Based on this, we reached the following empirical findings:

316 (1) Within the DeepLab series, the DeepLabV3+ model using ResNet101 as the backbone outperformed other variants in  
317 capturing water surface edges and shadow details. However, when compared to the NWseg model, there remains a  
318 considerable performance gap.

319 (2) The NWseg, U-Net, and ResNet50-FCN models demonstrated excellent performance in recognizing large-scale  
320 flooded areas, effectively capturing the overall contours of flood zones and exhibiting strong generalization capabilities.  
321 Specifically, NWseg shows higher accuracy and robustness in complex scene tests, while ResNet50-FCN and U-Net have  
322 some deficiencies and false detections in detecting edge details. In contrast, the lightweight LRASPP model showed limited  
323 ability to recognize flooded areas in nighttime scenes, resulting in relatively poor performance.



324 (3) Through examining each model in complex scenes, we validated the NWseg model's effectiveness and stability in  
325 diverse environments and conditions.

326 This study successfully demonstrates the superior performance of the NWseg model in nighttime urban flood  
327 detection (Wan et al., 2024). However, the model's decoupling and parsing process involves complex decomposition of  
328 lighting components and adaptive fusion, leading to high computational resource demands, which may impact its  
329 practical usability. Future work will focus on reducing the model's parameters and computational costs while  
330 maintaining accuracy. Additionally, further optimization of the dataset and model improvements will be pursued to  
331 enhance the overall performance of the NWseg model, broadening its potential applications.

332 **Data availability.** Data will be made available on request.

333 **Author contributions.** Xing Wang, Jiaquan Wan, Yannian Cheng, Cuiyan Zhang: Writing – original draft, Validation,  
334 Software, Methodology, Investigation. Xing Wang, Jiaquan Wan, Yannian Cheng: Writing – review & editing,  
335 Validation. Tao Yang: Writing – review & editing, Supervision. Fengchang Xue: Formal analysis, Validation. Yufang  
336 Shen: Data curation, Validation. Quan J. Wang: Data curation, Validation.

337 **Competing interests.** The contact author has declared that none of the authors has any competing interests.

## 338 **References**

- 339 Bai, G., Hou, J., Han, H., Xia, J., Li, B., Zhang, Y., and Wei, Z.: Intelligent monitoring method for road inundation based on deep learning,  
340 *Water Resources Protection*, 37, 75-80, 2021.
- 341 Cheng, Y., Gu, Q., Wang, Z., and Li, Z.: Wood Defect Image Segmentation Based on Deep Learning, *FORESTRY MACHINERY &*  
342 *WOODWORKING EQUIPMENT*, 46, 33-36, <http://doi.org/10.13594/j.cnki.mcjgjx.2018.05.004>, 2018.
- 343 Chen, C., Hao, X., Long, H., and Sun, X.: Asphalt Road Crack Detection Method Based on Improved DeepLabv3+ Network,  
344 *SEMICONDUCTOROPTOELECTRONICS*, 45, 493-500, <http://doi.org/10.16818/j.issn1001-5868.2023103002>, 2024.
- 345 Feng, T., Guo, Y., Huang, X., and Qiao, Y.: Cattle Target Segmentation Method in Multi-Scenes Using Improved DeepLabV3+ Method,  
346 *Animals*, 13, 2521, <http://doi.org/10.3390/ani13152521>, 2023.
- 347 Gao, F.: Urban Flood Disaster Risk Factor Identification Based on Deep Learning MBA thesis, Changzhou University, Changzhou,  
348 <http://doi.org/10.27739/d.cnki.gjsgy.2023.000080>, 2023.
- 349 Hao, Y.: Urban Flood Disaster Risk Warning Based on Deep Learning MBA thesis, Changzhou University, Changzhou,  
350 <http://doi.org/10.27739/d.cnki.gjsgy.2022.000104>, 2022.
- 351 Jin, K., Zhang, J., Wang, Z., Zhang, J., Liu, N., Li, M., and Ma, Z.: Application of deep learning based on thermal images to identify the  
352 water stress in cotton under film-mulched drip irrigation, *Agricultural Water Management*, 299, 108901,  
353 <http://doi.org/10.1016/j.agwat.2024.108901>, 2024.
- 354 Jin, N.: Research on Passible Area Detection Based on Deep Learning for All Types of Roads in both Fog and Sunny Conditions MEng  
355 thesis Sichuan University, Chengdu, <http://doi.org/10.27342/d.cnki.gscedu.2023.001503>, 2023.



- 356 Luo, H.: A Study on Risk Assessment Method of Urban Flood Disaster and Its Applications, MSc thesis, South China University of  
357 Technology, Guangzhou, <http://doi.org/10.27151/d.cnki.gnhlu.2020.002269>, 2020.
- 358 Liao, Y.: Research on recognition method of urban road waterlogging information based on deep learning MEng thesis, South China  
359 University of Technology, Guangzhou, <http://doi.org/10.27151/d.cnki.gnhlu.2023.004803>, 2023.
- 360 Li, F., Shi, J., Liang, X., Li, Y., Liu, P., and Chen, X.: Research on Hilly Field Road Image Segmentation Method Based on Improved  
361 DeepLabV3+, *Journal of Southwest University (Natural Science Edition)*, 46, 172-183,  
362 <http://doi.org/10.13718/j.cnki.xdzk.2024.08.016>, 2024.
- 363 Li, B.: Research on forestland classification based on improved DeepLabV3+, MSc thesis, Central South University of Forestry and  
364 Technology, Changsha, <http://doi.org/10.27662/d.cnki.gznlc.2024.000886>, 2024.
- 365 Liang, Y., Li, X., Tsai, B., Chen, Q., and Jafari, N.: V-FloodNet: A video segmentation system for urban flood detection and quantification,  
366 *Environmental Modelling & Software*, 160, 105586, <http://doi.org/10.1016/j.envsoft.2022.105586>, 2023.
- 367 Ma, J., Guo, Z., Ma, Z., Ma, X., and Li, J.: Remote sensing image land fesarure segmentation method based on lightweight DeepLabV3+,  
368 *Chinese Journal of Liquid Crystals and Displays*, 39, 1001-1013, 2024.
- 369 Peng, H., Xiang, S., Chen, M., Li, H., and Su, Q.: DCN-Deeplabv3+: A Novel Road Segmentation Algorithm Based on Improved  
370 Deeplabv3+, *Ieece Access*, 12, 87397-87406, <http://doi.org/10.1109/access.2024.3416468>, 2024.
- 371 Sarp, S., Kuzlu, M., Cetin, M., Sazara, C., and Guler, O.: Detecting floodwater on roadways from image data using Mask-R-CNN, 2020  
372 International Conference on INnovations in Intelligent SysTems and Applications, Novi Sad, Serbia, 24-26 August 2020,  
373 <http://doi.org/10.1109/INISTA49547.2020.9194655>.
- 374 Sazara, C., Cetin, K., and Iftekharuddin, K.: Detecting floodwater on roadways from image data with handcrafted features and deep  
375 transfer learning, 2019 IEEE Intelligent Transportation Systems Conference, Auckland, New Zealand, 27-30 October 2019,  
376 <http://doi.org/10.1109/ITSC.2019.8917368>.
- 377 Tao, L.: Research on Road Scene Semantic Segmentation Method Based on DeepLabV3+ Model, MEng thesis, Dalian Jiaotong University,  
378 Dalian, <http://doi.org/10.26990/d.cnki.gsltc.2023.000111>, 2023.
- 379 Tan, X., Xu, K., Cao, Y., Zhang, Y., Ma, L., and Lau, RWH.: Night-Time Scene Parsing With a Large Real Dataset *Ieece Transactions on*  
380 *Image Processing*, 30, 9085-9098, <http://doi.org/10.1109/tip.2021.3122004>, 2021.
- 381 Tang, Y., Tan, D., Li, H., Zhu, M., Li, X., Wang, X., Wang, J., Wang, Z., Gao, C., Wang, J., and Han, A.: RTC\_TongueNet: An improved  
382 tongue image segmentation model based on DeepLabV3 *DIGITAL HEALTH*, 10, 20552076241242773,  
383 <http://doi.org/10.1177/20552076241242773>, 2024.
- 384 Wan, J., Qin, Y., Shen, Y., Yang, T., Yan, X., Zhang, S., Yang, G., Xue, F., and Wang, Q.: Automatic detection of urban flood level with  
385 YOLOv8 using flooded vehicle dataset, *Journal of Hydrology*, 639, 131625, <http://doi.org/10.1016/j.jhydrol.2024.131625>, 2024.
- 386 Wang, Y., Shen, Y., Salahshour, B., Cetin, M., Iftekharuddin, K., Tahvildari, N., Huang, G., Harris, D., Ampofo, K., and Goodall, J.:  
387 Urban flood extent segmentation and evaluation from real-world surveillance camera images using deep convolutional neural network,  
388 *Environmental Modelling & Software*, 173, 105939, <http://doi.org/10.1016/j.envsoft.2023.105939>, 2024.
- 389 Wang, H., Cai, B., Cai, Y., Liu, Z., Sun, K., and Chen, L.: Detection of Water covered and Wet Areas on Road Pavement Based on  
390 Semantic Segmentation Network, *Automotive Engineering*, 43, 485-491, <http://doi.org/10.19562/j.chinasae.qcgc.2021.04.005>, 2021.
- 391 Wei, Z., Chen, L., Tu, T., Ling, P., Chen, H., and Jin, Y.: Disentangle then Parse: Night-time Semantic Segmentation with Illumination  
392 Disentanglement, *Proceedings of the IEEE/CVF International Conference on Computer Vision (ICCV)*, 21593-21603,  
393 <https://doi.org/10.48550/arXiv.2307.09362>, 2023.
- 394 Wang, Z.: Semantic segmentation-based waterlogged region recognition model and application research, MEng thesis, Institute of Disaster  
395 Prevention, Sanhe, <https://doi.org/10.27899/d.cnki.gfzkj.2024.000003>, 2024.
- 396 Xue, F., Lv, X., and Chen, X.: Urban flood monitoring method based on improved DeeplabV3+, *Science of Surveying and Mapping*, 48,  
397 216-224, <http://doi.org/10.16251/j.cnki.1009-2307.2023.10.022>, 2023.
- 398 Yang, Y.: Research on Multispectral Retinal Image Segmentation Based on Convolutional Neural Network, MEng thesis, Hebei  
399 University, Baoding, <http://doi.org/10.1016/10.27103/d.cnki.ghebu.2023.001067>, 2023.



- 400 Yadavendra, and Chand, S.: Semantic segmentation of human cell nucleus using deep U-Net and other versions of U-Net models,  
401 Network-Computation in Neural Systems, 33, 167-186, <http://doi.org/10.1080/0954898x.2022.2096938>, 2022.
- 402 Yang, K., Zhang, S., Yang, X., and Wu, N.: Flood Detection Based on Unmanned Aerial Vehicle System and Deep Learning, Complexity,  
403 2022, 6155300, <http://doi.org/10.1155/2022/6155300>, 2022.
- 404 Zhang, T., Wang, D., and Lu, Y.: ECSNet: An Accelerated Real-Time Image Segmentation CNN Architecture for Pavement Crack  
405 Detection, Ieee Transactions on Intelligent Transportation Systems, 24, 15105-15112, <http://doi.org/10.1109/tits.2023.3300312>, 2023.
- 406 Zhang, J.: Research on Citrus Segmentation Algorithm Based on Improved DeepLabv3+, MEng thesis, Shaanxi University of Technology,  
407 Xian, <http://doi.org/10.27733/d.cnki.gsxlq.2024.000066>, 2024.
- 408 Zhang, Y., Wang, H., Liu, J., Zhao, X., Lu, Y., Qu, T., Tian, H., Su, J., Luo, D., and Yang, Y.: A Lightweight Winter Wheat Planting Area  
409 Extraction Model Based on Improved DeepLabv3+and CBAM, Remote Sensing, 15, 4156, <http://doi.org/10.3390/rs15174156>, 2023.
- 410 Zhao, W., Zhang, H., Yan, Y., Fu, Y., and Wang, H.: A Semantic Segmentation Algorithm Using FCN with Combination of BSLIC,  
411 Applied Sciences-Basel, 8, 500, <http://doi.org/10.3390/app8040500>, 2018.